

CONTACT STRESSES BETWEEN TWO CYLINDRICAL BODIES WITH PARALLEL AXES: ANALYSIS BY F.E.M.

Ligia Cristina BREZEANU
“Petru Maior” University of Tîrgu Mureș
Nicolae Iorga Street, no.1, Tîrgu Mureș, Romania
ligia.brezeanu@ing.upm.ro

Abstract

This paper presents an analysis of the stresses and deformations occurring upon contact between two bodies under compression strain, using the Finite Element Method (FEM). The results are compared to the results obtained by using calculations according to the theory of H. Hertz.

The analyzed situation is that where two cylindrical bodies with parallel axes are in contact both having the same radius R .

Keywords: contact stresses, cylinders with parallel axes, stresses, displacements

1. Introduction

Contact stresses occur in the transmission of forces between two parts with punctiform contact: roller bearings or ball bearings, toothed gears, cam mechanisms, etc.

On basis of the general equations of the theory of elasticity, H. Hertz (1881-1882) laid the foundations of the theory of stresses and deformations of elastic bodies in contact points.

In the general case of two bodies in contact subjected to a perpendicular force on the contact surfaces the outline of the contact surface is an ellipsis, which transforms into a circular surface or a strip in extreme situations (the case of linear contact can be considered a particular case of the punctiform contact).

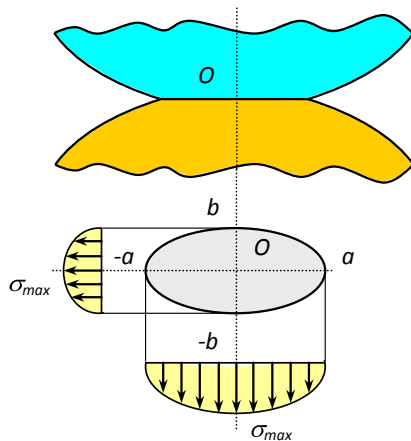


Fig.1: Contact between two bodies [2]

The distribution of the stress on the contact surface is given by the ordinates of the ellipsoid built on the contact surface with the maximum stress at the centre of the ellipsis (Fig.1).

The material in the vicinity of the contact ellipsis is compressed in all directions approximately identically and can withstand to high stresses without residual deformations. Thus, experiments show that for special steels for rolling bodies in punctiform contact in use, the allowable value of the maximum stress is [10]:

$$\sigma_a^* = 3500 \div 5000 \text{ MPa - for steel}$$

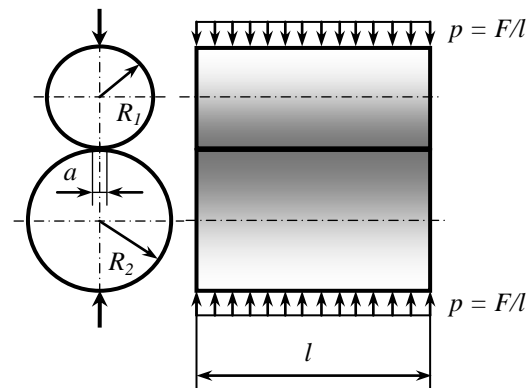


Fig.2: Contact between two cylinders with parallel axes

Given two cylindrical bodies in contact with radii R_1 and R_2 , compressed by a uniformly distributed force $p = F/l$, the contact between the cylinders occurs following parallel generating lines and the contact area is shaped like a rectangular figure (Fig. 2, Fig. 3).

Normal compression stresses on the contact area is spread over a semi-cylinder (Fig.3.).

The width of the rectangular contact area “ a ”, if: $E_1 = E_2 = E$, by [7] and [10]:

$$\alpha = 1.522 \sqrt{\frac{F}{l \cdot E} \cdot \frac{R_1 \cdot R_2}{R_1 + R_2}} \quad (1)$$

For: $R_1 = R_2 = R$

$$\alpha = 1.076 \sqrt{\frac{F \cdot R}{l \cdot E}} \quad (2)$$

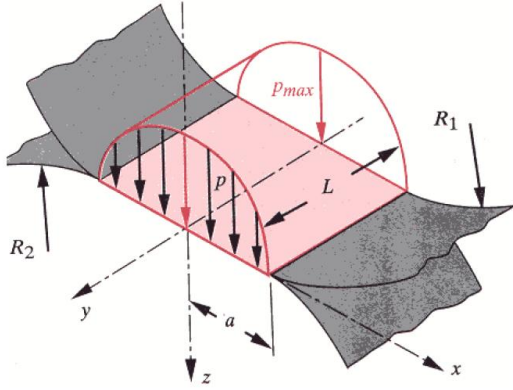


Fig. 3: Distribution of stresses in the contact area of two cylindrical bodies with parallel axes

The maximum stress is in the contact centre and is determined by the relation, if $E_1 = E_2 = E$:

$$\sigma_{\max} = 0.418 \sqrt{\frac{F \cdot E}{l} \cdot \frac{R_1 + R_2}{R_1 \cdot R_2}} \quad (3)$$

For: $R_1 = R_2 = R$

$$\sigma_{\max} = 0.591 \sqrt{\frac{F \cdot E}{l \cdot R}} \quad (4)$$

The most dangerous point in the contact area is found on axis “ z ”, at a depth of $\approx 0.4 a$.

The main stresses in this point are:

$$\begin{cases} \sigma_1 = -0.180 \sigma_{\max} \\ \sigma_2 = -0.288 \sigma_{\max} \\ \sigma_3 = -0.780 \sigma_{\max} \end{cases} \quad (5)$$

The maximum tangential stress in the most dangerous point is:

$$\tau_{\max} = 0.3 \sigma_{\max} \quad (6)$$

To make a comparison the same values can be calculated correspondingly [13]: Wikipedia- Contact mechanics,

[http://www.wikipedia.org/wiki/contact_mechanics:](http://www.wikipedia.org/wiki/contact_mechanics)

$$\sigma_{\max} = 0.591 \sqrt{\frac{F \cdot E^*}{\pi \cdot l \cdot R}} \quad (7)$$

Where:

$$\frac{1}{E^*} = \frac{1 - \mu_1^2}{E_1} + \frac{1 - \mu_2^2}{E_2} \quad (8)$$

$$\frac{1}{R} = \frac{1}{R_1} + \frac{1}{R_2} \quad (9)$$

The width of the rectangular contact area “ a ”,

$$a = \sqrt{R \cdot d} \quad (10)$$

where, indentation depth “ d ” is :

$$d = \frac{4 F}{\pi \cdot E^* \cdot l} \quad (11)$$

In contact between two cylinders with parallel axes, the force is linearly proportional to the indentation depth.

Control of the strength of contact stresses

Condition for working stress, corresponding strength theories III (Tresca) or IV (Von Mises):

$$\sigma_{ech III} = \sigma_1 - \sigma_3 \leq |\sigma_a| \quad (12)$$

or:

$$\sigma_{ech IV} = \sqrt{\frac{1}{2} \left(\sigma_1 - \sigma_2 \right)^2 + \left(\sigma_2 - \sigma_3 \right)^2 + \left(\sigma_3 - \sigma_1 \right)^2} \leq |\sigma_a| \quad (13)$$

Calculating σ_{\max} in the centre of the contact area we can write the strength condition:

$$\sigma_{ech} = m \cdot \sigma_{\max} \leq |\sigma_a| \quad (14)$$

- σ_{ech} expressed on basis of strength theories, III, or IV (15, 16).

From where:

$$\sigma_{\max} \leq \frac{1}{m} |\sigma_a| = |\sigma_a^*| \quad (15)$$

where:

- $|\sigma_a^*|$ - is the allowable value of the maximum stress

in the contact centre;

- m coefficient in function of rapport a/b (table 2)

- a, b the dimensions of the contact area (Fig.1.).

Table 2. Value of coefficient m [10]

$\frac{b}{a}$	$m = \frac{\sigma_{ech III}}{\sigma_{\max}}$	$m = \frac{\sigma_{ech IV}}{\sigma_{\max}}$
0 (band)	0,600	0,557

2. Materials and Methods

The analysis of stresses and deformations was made using the FEM (Finite Element Method) [1], [3]-[6], [8]-[9]. The results obtained were compared to those calculated according to [7], [10], and [13]-[15].

Modeling, simulations and FEM analysis was made in the ALGOR V16 Fempro software [12].

Finite elements used are 3D type – brick. For the model: two cylinders with parallel axes, after meshing result (Fig.4):

- $R_1 = R_2 = 5\text{ mm}$; $l = 30\text{ mm}$;
- Number of nodes : 32277
- Number E.F.- type 3D: 30720

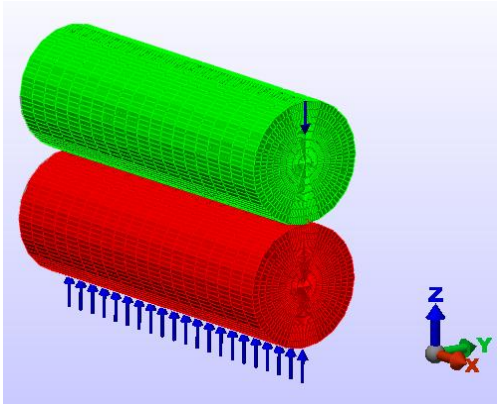


Fig. 4: Contact between two cylinders with parallel axes: Modeling and meshing

The contact between the bodies is bonded. The value of nodal force acting in the contact point is: $p = F/l : 100\text{ N/mm}$.

The bodies in contact are made of steel and the mechanical properties of the materials are:

- $E = 2,1 \cdot 10^5\text{ MPa}$ – Young’s modulus;
- $\mu = 0,3$ – Poisson’s ratio.

3. Results

The results are considered to be significant for the interpretation and relevance given the phenomenon studied is the values:

- Equivalent stress Von Mises σ_{ech} ;
- Minimum principal stress σ_3 (with compression effect);
- Intermediate principal stress σ_2 (with compression effect);
- Maximum principal stress σ_1 (with compression effect);
- Shear stress τ ;
- Displacement in contact point and in dangerous point

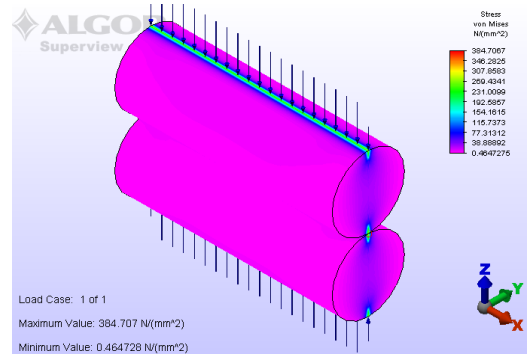


Fig. 5: Equivalent stress Von Mises σ_{ech} distribution in two cylinders

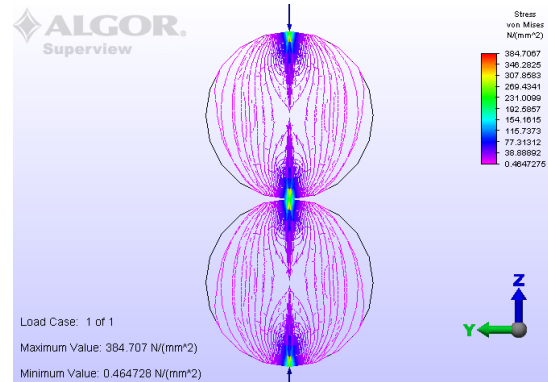


Fig. 6: Equal stress Von Mises σ_{ech} distribution in cross-section area of two cylinders

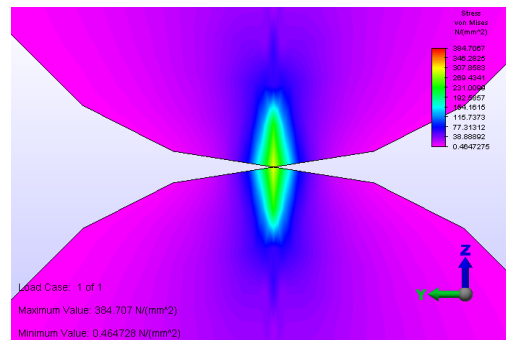


Fig. 7: Detail – Equivalent stress Von Mises σ_{ech} distribution in contact area of the two cylinders

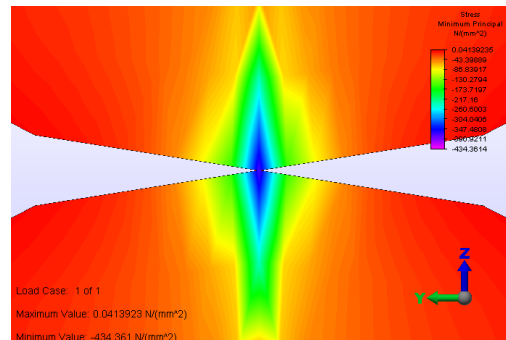


Fig. 8: Detail - Minimum principal stress σ_3 distribution in contact area of the two cylinders

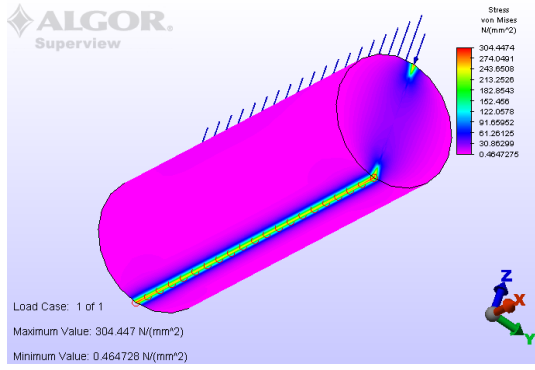


Fig. 9: Equivalent stress Von Mises σ_{ech} distribution in the upper cylinder

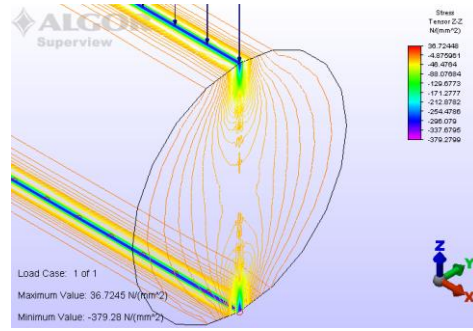


Fig. 13: Detail - Equal stress: Minimum principal σ_z distribution in the upper cylinder

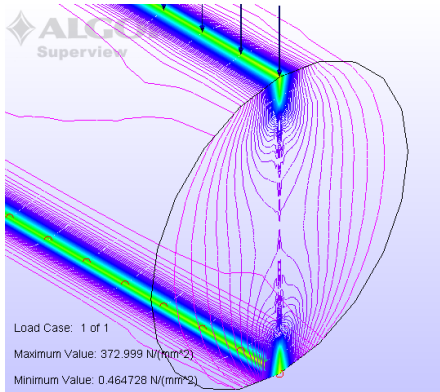


Fig. 10: Detail - Equal stress Von Mises σ_{ech} distribution in the upper cylinder

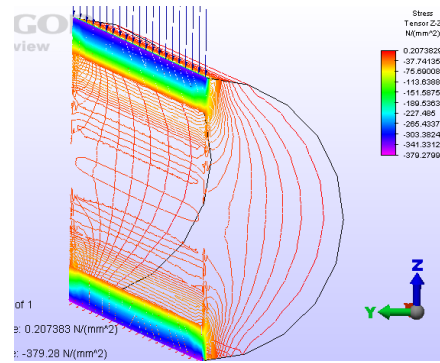


Fig. 14: Detail - Equal stress: Minimum principal σ_3 distribution in the upper cylinder

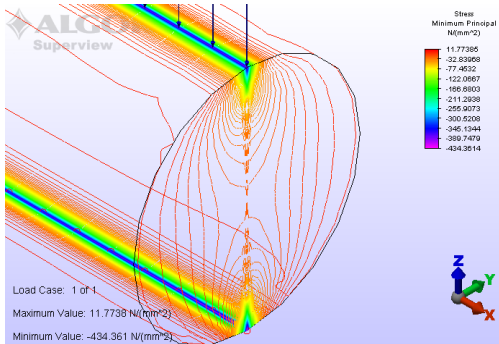


Fig. 11: Detail - Equal stress: Minimum principal σ_3 distribution in the upper cylinder

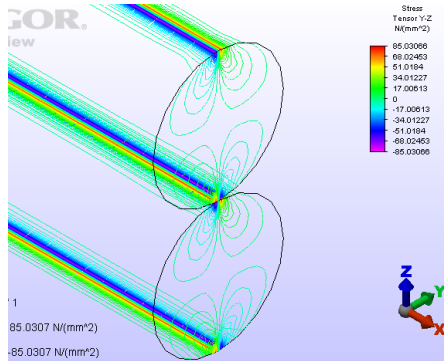


Fig. 15: Detail - Shear stress τ distribution in the upper cylinder

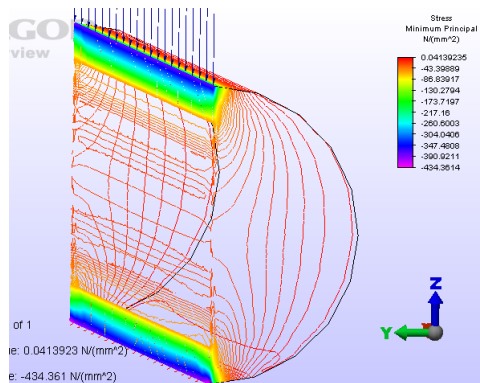


Fig. 12: Detail - Equal stress: Minimum principal stress σ_3 distribution in the upper cylinder cross-section

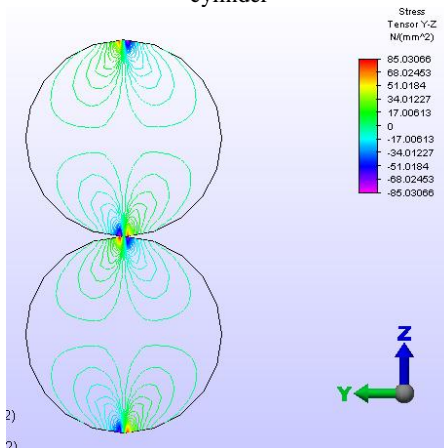


Fig. 16: Detail - Shear stress τ distribution in the upper cylinder

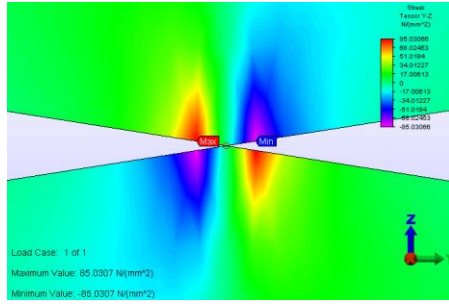


Fig. 17: Detail - Shear stress τ distribution in the contact area of the two cylinders

Table 2: Values of the stress and displacements - Contact between two cylinders with parallel axes

Values		The contact point	
		FEM	Calc.
σ_{max} (4)	[MPa]	-371.47	-1211.19
σ_{max} (7)			-1210.36
σ_{max} [14]			-1212.07
$\sigma_{ech} = m \cdot \sigma_{max}$ (14), (4), (7)		384.71	726.71
σ_1		-106.29	-
σ_2		-171.62	-
σ_3		-434.36	-
σ_z		-379.28	-
τ		0	0
a (2)		[mm]	-
a (10)	0.0744		
a [14]	0.0525		
δ_z (11)		0.00084	0.00111
δ_z [12]			0.0042
Values		In the most dangerous point : $z \approx 0,4 a$	
		FEM	Calc.
τ_{max} (6)	[MPa]	-85.03	± 363.36
σ_1 (5)		-99.73	-218.00
σ_2 (5)		-141.39	-348.82
σ_3 (5)		-371.47	-944.73

The values obtained after the simulations for contact between two cylinders with parallel axes, and the values obtained corresponding to relations (2), (4), (5), (6), (14) after [7], [10] and (7), (8), (9), (10), (11), after [14] are contained in table 1.

The values calculated with the relations (4) and (7) correspond with those calculated with [14], [15].

4. Discussion

Following the FEM analysis we note:

- The distributions of maximum stresses on the contact surface follows a rectangular strip (Fig.9, Fig.10, Fig.11., Fig.13);
- The distribution of stresses in the section perpendicular to the axes of the two cylinders is approximately a semi-cylinder with maximum in the contact area (Fig.6., Fig.7., Fig.8., Fig.9., Fig.10., Fig.11.);
- The distribution of maximum stresses σ_{ech} , σ_3 and

σ_z , in a vertical section that contains the axes of the two cylinders and the contact generating line follows a rectangular strip (Fig.12., Fig.14.);

- The distribution of shear stresses is asymmetrical to the contact generating line (Fig.15., Fig.16., Fig.17.);
- The shear stresses in the contact points are non-existing;
- Maximum shear stresses are situated at points symmetrical to the contact generating line in the coordinate points: $y = 0.193154$ mm; $z = 0.0306$, at the depth $z \approx 0,4 a$ (Fig.15., Fig.16., Fig.17.);
- The stresses resulting from the FEM simulations have smaller values than those calculated (table 2);
- The stresses calculated with relations (4), (7), and [10] are quite close;
- All the stresses on the contact area and within the affected zone are compression stresses (table 2);

5. Conclusions

The FEM analysis confirms the existing theory referring to the contact stresses between two bodies under compression loads (H. Hertz). In the contact area appears a strong phenomenon of stress concentration, with values much higher than in the other bodies in contact.

The distribution of stresses in the contact area corresponds to the estimations according to the theoretical distribution.

Although the values obtained following the simulations are smaller than the calculated values, the rapport between these values is the same with that between the theoretical values.

References

- [1] Batoz, J.L. and Dhatt G. (1990), *Modelisation des structures par elements finis (Modelling of the structures with finites elements)*, Edition Hermes, Paris (in French).
- [2] Brezeanu, L.C. (2013), *Contact stresses: Analisis by finite element method (FEM)*, Procedia Technology, Vol.8, pp.401-410, <http://inter-eng.upm.ro/2012/proceedings.html>
- [3] Craveur, J.C. (2001), *Modelisation des structures (Modelling of the structures)*, Edition Dunod, Paris (in French).
- [4] Deeg, E.W. (1992), *New Algorithms for Calculating Hertzian Stresses, Deformations, and Contact zone Parameters*, AMP Journal of Technology, Vol.2, pp.14-24.
- [5] Jacob, E. (2011), *Tutorial Report on Hertzian Contact Stress Theory*, OPTI 521, College of Optical Sciences, University of Arizona, Tucson, AZ.
- [6] Nicholas, L.C. (2011), *Tutorial of Hertzian Contact Stress Analysis*, OPTI 521, College of Optical Sciences, University of Arizona, Tucson, AZ.
- [7] Mocanu, D.R. (1980), *Rezistenta materialelor (Strength of materials)*, Technical Edition, Bucharest, (in Romanian).

- [8] Vahid, M. (2011), *A new analytical formulation for contact stress and prediction of crack propagation path in rolling bodies and comparing with finite element model (FEM) results statically*, International Journal of the Physical Sciences, Vol.6 (15), pp.3589-3594.
- [9] Vahid, M.(2012), *Contact Stress Analysis in Rolling Bodies by Finite Element Method (FEM) Statically*, Journal of Mechanical Engineering and Automation, Vol.2 (2), pp.12-16.
- [10] Pissarenko, G, Yakovlev, A, Matveev, V. (1979) *Aide-memoire de resistance des materiaux (Help-memory, strength of materials)*, Edition Mir, Moscow (in French).
- [11] Tudose, I., Constantinescu, M.D. and Stoica M., (1990), *Rezistența materialelor (Strength of materials)*, Technical Edition, Bucharest, (in Romanian).
- [12] *** ALGOR: Finite element analysis in practice-Instructor manual, Algor Inc., Pittsburgh, USA, 2004.
- [13] *** Wikipedia: Contact mechanics [Online], Available: http://www.wikipedia.org/wiki/contact_mechanics
- [14] *** Calculation of contact stress, [Online]. Available: <http://www.mesys.ch/calc/hertz.fcgi>
- [15] *** Rolling contact phenomena : Hertzian line contact,[Online]. Available: <http://www.tribology-abc.com/calculators>
- [16] *** Tutorials on select topics in optomechanics, [Online].Available: <http://fp.optics.arizona.edu/optomech>